Journal of Materials Chemistry

Cite this: J. Mater. Chem., 2011, 21, 8066

www.rsc.org/materials

PAPER

High Pt loading on functionalized multiwall carbon nanotubes as a highly efficient cathode electrocatalyst for proton exchange membrane fuel cells†

Baizeng Fang,[abc] Min-Sik Kim,[a] Jung Ho Kim,[a] Min Young Song,[a] Yan-Jie Wang,[bc] Haijiang Wang,*[d] David P. Wilkinson*[bcd] and Jong-Sung Yu*[a]

Received 25th February 2011, Accepted 22nd March 2011
DOI: 10.1039/c1jm10847f

A very efficient, reproducible approach has been developed to fabricate a multiwall carbon nanotube (MWCNT)-supported, high Pt loading electrocatalyst. In this strategy, MWCNT was first functionalized with an anionic surfactant, sodium dodecylsulfate (SDS), to enhance the hydrophilicity of the MWCNTs for high Pt loading. The SDS-modified MWCNTs were further used to support high loading of Pt nanoparticles (NPs) through a urea-assisted homogeneous deposition (HD) strategy, followed by reduction using ethylene glycol (EG) as the precursor of a reducing agent. Through the input of SDS on the MWCNTs, Pt complex species can be readily anchored on the outer surface of the MWCNTs, while *in situ* pH adjustment of the solution with urea and reduction by EG enable the Pt NPs to disperse very uniformly on the SDS–MWCNT support with small particles size. Due to its unique structural characteristics, such as high electronic conductivity, the one-dimensional nanotube structure favouring fast electron transfer and more uniform Pt NP dispersion on the support with smaller particle size, the SDS-MWCNT-supported Pt (60 wt%) catalyst considerably outperformed a commercially available Johnson Matthey catalyst with the same Pt loading supported on Vulcan carbon black, when they were each employed as a cathode catalyst in proton exchange membrane fuel cells.

1. Introduction

Proton exchange membrane fuel cells (PEMFCs) represent the most advanced fuel-cell technology. They have been of great interest as future energy sources for various applications, such as low/zero-emission electric vehicles, distributed home power generators and power sources for small portable electronics. This is because of their high power density, relatively quick start-up, rapid response to varying the loading, and relatively low operating temperature.[1–5] However, the commercial viability of the PEMFC technology has been hindered by several challenges, including poor kinetics of the oxygen reduction reaction (ORR) and the high cost of noble metal (*i.e.*, Pt) catalysts.

Catalyst support technology has been proved to be an effective approach to lower the usage of noble metals in catalysts and, meanwhile, to improve the catalytic activity of the supported catalysts.[6–11] Catalyst supports play a very important role in distributing and stabilizing the catalyst particles, determining the size, dispersion degrees, alloy degree of the catalyst and the diffusion kinetics of the reactants and products in the catalytic system. Thus, synthesis of supported Pt-based NPs with a uniform size and good dispersion on their support is paramount.

Carbon black Vulcan XC-72 (VC) has been widely used as an electrocatalyst support in low temperature fuel cells due to its relatively large surface area and excellent chemical stability in the fuel cell environment. However, approximately 47% of carbon black VC is comprised of micropores,[12] some of which are too small (less than 1 nm in diameter) to be accessible to the electrolyte polymer, resulting in the entrapped Pt NPs not contributeing to the electrode reactions due to the absence of the triple-phase boundaries (*i.e.*, gas–electrolyte–electrode). Some novel nanostructured carbon materials have recently been investigated as possible catalyst supports for PEMFCs, including carbon nanotubes (CNTs)[13–16] and carbon nanofibers (CNFs).[17–19] More recently, hierarchically nanostructured carbon materials, such as

[a]*Department of Advanced Materials Chemistry, WCU Research Team, Korea University, 208 Seochang, Jochiwon, ChungNam, 339-700, Republic of Korea. E-mail: jsyu212@korea.ac.kr; Fax: (+81)-41-867-5396*
[b]*Department of Chemical & Biological Engineering, University of British Columbia, 2360 East Mall, Vancouver, B. C., Canada V6T 1Z3. E-mail: dwilkinson@chbe.ubc.ca*
[c]*Clean Energy Research Centre, 2360 East Mall, Vancouver, B. C., Canada V6T 1Z3*
[d]*Institute for Fuel Cell Innovation, National Research Council Canada, 4250 Wesbrook Mall, Vancouver, B.C., Canada V6T 1W5. E-mail: haijiang.wang@nrc.gc.ca*

† Electronic supplementary information (ESI) available: TGA for MWCNTs and SDS–MWCNTs, various MWCNT-supported Pt catalysts, TEM images and XRD for SDS-MWCNT supported Pt(60 wt%). See DOI: 10.1039/c1jm10847f

hollow spherical carbon with a mesoporous shell and ordered multimodal porous carbon, have been investigated as catalyst supports.[20,21] Although these hierarchically nanostructured carbon materials have demonstrated superb performance when they were employed as catalyst supports compared with carbon black VC supported Pt-based catalysts, their syntheses are generally complicated and time-consuming and, at present, they are produced in laboratories on a small scale. In contrast, CNTs not only have a high surface area and chemical stability but also have excellent mechanical and electronic properties and particularly abundant CNTs are commercially available at a relatively low cost, making them potential competitive candidates for use as catalyst supports. Although the CNT-supported Pt electrode revealed a higher power density than the VC-supported one,[13] the realistic application of CNTs as cathode catalyst supports has been greatly hindered by several difficulties associated with processes for their purification and dispersion, particularly in supporting high loading of noble metals (*i.e.*, Pt) with a uniform distribution of Pt NPs.

To date, various synthetic strategies have been developed to fabricate supported catalysts, such as the impregnation method with $NaBH_4$ as a reducing agent,[22] colloidal methods,[23,24] microemulsion methods,[25] a microwave-assisted ethylene glycol (EG) process,[26,27] γ-ray irradiation,[28] urea-assisted homogeneous deposition HD-EG[29] and urea-assisted HD-H_2.[30] Although these methods have been widely used in catalyst syntheses and some of them have been proven to be very effective in preparing VC-supported Pt catalysts, there is great difficulty in preparing CNT-supported Pt catalysts with high metal loading because pristine CNTs are chemically inert, which make it difficult to anchor and deposit Pt NPs without the activation of the graphitic surface. So far, much effort has been made toward creating defect sites in CNTs and/or improving the hydrophilicity of CNTs in order for CNTs to support high loading of the metal catalyst (*i.e.*, Pt). Post-synthesis treatments of CNTs, such as chemical oxidation by strong acids[31,32] and sono-chemical treatment,[33] have been commonly used to introduce defect sites into CNTs for improved deposition of precious metals on the CNT supports. However, the introduction of a large number of defects may reduce the electrical conductivity and corrosion resistance of CNTs, resulting in a loss in the electrochemical surface area (ECSA) of the supported Pt NPs and reduced durability during fuel cell operation.[34] Recently, non-covalent functionalization of CNTs has attracted particular attention. This enables the properties of the hybrids of metal NPs and CNTs to be tailored, while still preserving the intrinsic properties of the CNTs.[35] These approaches mainly include functionalizing CNTs with surfactants, such as polyaniline (for Au loading),[36] cetyltrimethylammonium bromide,[37] 1-aminopyrene,[35] poly (diallyldimethylammonium chloride),[38] sodium dodecyl sulfate (SDS),[39] ionic-liquid polymer[40] and the more recently developed solvent-free high temperature activation strategy.[41] Impressively, SDS could not only modify the surface structure of CNTs but also acted as the reducing and protective agents for the deposition of Pt metal, and, in this case, there was no need for an external reducing agent.[39] The reducing agent 1-dodecanol could be produced *in situ* through the gradual decomposition of SDS at an elevated temperature (*i.e.* 130 °C).[42] However, some problems may arise upon the synthesis of a CNT-supported catalyst with high Pt loading, for which a large quantity (*i.e.* an excess) of reducing agent (*i.e.* SDS) will be required and, in this case, the interaction of Pt(IV) species with SDS not only takes place on the outer surface of the CNTs "coated" by SDS, but also in the bulk solution containing a large amount of the remaining SDS. Therefore, the reduction of the Pt complex species will proceed not only on the CNT support but also in the bulk solution, and thus it is impossible to realize a homogeneous deposition of Pt NPs on the CNTs support. To solve this problem, an external reducing agent is necessary.

In this study, a novel and very efficient synthesis strategy was developed, which is illustrated in Scheme 1. It is evident that this synthetic strategy combines the advantage of using SDS as a non-covalent stabilizer to improve the adsorption of Pt(IV) species on the mutiwall CNT support and the advantages of a urea-assisted HD-EG process, namely, *in situ* pH adjustment and homogeneous deposition of the Pt complex species on the MWCNT support through the gradual hydrolysis of urea at 353 K and through the *in situ* reduction of the Pt species by EG at an elevated temperature (*i.e.*, 393 K). It has been reported that ensuring the optimum pH is particularly important to ensure the reproducibility of the surfactant-based method, which is a basic requirement for a good Pt dispersion on the CNT support.[43] To investigate the effects of SDS, the pH and the reducing agent, various synthetic strategies were examined, such as the HD-EG strategy[29] for the MWCNTs without SDS treatment, SDS as the reducing agent,[39] the impregnation method using $NaBH_4$ as a reducing agent for the SDS–MWCNTs, microwave-assisted EG at pH = 8, and a HD-EG strategy for the SDS-MWCNTs. Evidently, the Pt (40 wt%)/SDS–MWCNT synthesized by the HD-EG strategy not only has higher Pt loading but also a more uniform distribution of the Pt NPs, along with smaller particle size. Furthermore, compared to the commercially available VC-supported Pt (60 wt%) catalyst from Johnson Matthey, the Pt (60 wt%)/SDS–MWCNT (HD-EG) catalyst demonstrated a more uniform dispersion of the Pt NPs on the support and a considerably improved PEMFC performance when they were each employed as the cathode catalyst.

2. Experimental section

2.1. Synthesis of MWCNT-supported high Pt loading catalysts

MWCNT-supported high Pt loading (40 or 60 wt%) catalysts were prepared through an innovative synthesis strategy combining a step for the surface functionalization of the MWCNTs and urea-assisted HD-EG steps for the homogeneous deposition and reduction of the Pt(IV) complex species. A typical

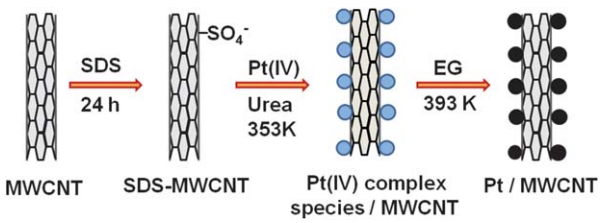

Scheme 1 A schematic diagram for the synthesis of a SDS–MWCNT-supported Pt catalyst using a urea-assisted HD-EG strategy.

synthesis is illustrated in Scheme 1. In this synthesis, SDS was employed in the first step for the non-covalent functionalization of the MWCNTs for improved adsorption of the Pt(IV) species on the support, while the following urea-assisted HD step allows *in situ* gradual pH adjustment through the hydrolysis of urea at 353 K and homogeneous deposition of the Pt(IV) complex species on the MWCNT support at the same temperature. The EG step ensures *in situ* homogenous reduction of the Pt(IV) complex species deposited on the MWCNT support by the reducing agent generated *in situ* from the decomposition of EG at 393 K. A typical synthesis of the SDS–MWCNT-supported (*i.e.* SDS-modified MWCNT) Pt catalysts using a urea-assisted HD-EG strategy is as follows. 100 mg MWCNTs (EMP, Korea) were suspended in 400 mL of 0.25 M SDS aqueous solution, then this was ultrasonicated for 1 h and stirred for 24 h. The solution was then filtrated and washed several times to remove the free SDS in the solution, followed by drying in a vacuum oven at 80 °C for 24 h. An appropriate amount of SDS–MWCNT (*i.e.*, 73.2 mg for Pt (40 wt%)/C and 32.5 mg for Pt (60 wt%)/C) was suspended in 300 mL deionised (DI) water containing 300 mg urea and this was sonicated for 30 min. Then, 5 mL of a 0.05M $H_2PtCl_6 \cdot 6H_2O$ aqueous solution was added. After stirring for 3 h, the solution was heated to 80 °C and this was kept constant for 3 h for complete hydrolysis of the urea. Next, 200 mL of EG was added and stirred for 3 h. The solution was heated to 120 °C and this was kept constant for 2 h. After stirring overnight, the catalyst slurry was filtrated and washed with a copious amount of DI water. The resultant Pt catalyst was dried at 80 °C overnight.

To investigate the effects of the pH and reducing agent on the dispersion and size of Pt NPs, other different synthetic strategies were also employed for the preparation of SDS–MWCNT-supported Pt(40 wt%) catalysts, including the impregnation method using $NaBH_4$ as a reducing agent at pH = 8 and a microwave assisted EG process at pH = 8. The synthesis details can be seen in our previous paper, where VC was used as the catalyst support.[29]

In the case of using SDS as an *in situ* reducing agent, a similar method to that reported by Lee *et al.*[39] was employed. Namely, 73.2 mg of MWCNTs were suspended in 750 mL of a 0.1 M SDS aqueous solution and sonicated for 4 h, followed by a reflux in an oil bath (130 °C) for 7 h. Next, 5 mL of a 0.05M $H_2PtCl_6 \cdot 6H_2O$ aqueous solution was added and stirred for 3 h. After cooling down, the catalyst slurry was filtrated and washed with copious amount of DI water, and the residue was dried at 80 °C overnight.

2.2. Surface characterization of MWCNT-supported Pt catalysts

The weight percentage of SDS in the SDS–MWCNTs and the Pt content (*i.e.* loading) in various MWCNT-supported Pt catalysts were roughly estimated using a thermal gravity analyzer (TGA 1000, SCINCO, Korea), which was performed at a heating rate of 10 °C min^{-1} in an N_2 atmosphere for SDS in SDS–WMCNT and in air for various MWCNT-supported Pt catalysts.

The dispersion of Pt NPs on the support in various MWCNT-supported Pt catalysts was characterized using scanning electron microscopy (SEM) and transmission electron microscopy (TEM). SEM images were obtained using a Hitachi S-4700 microscope operated at an acceleration voltage of 10 kV, and TEM analysis was operated on an EM 912 Omega microscope at 120 kV. High-resolution TEM (HRTEM) images were obtained on a JEOL FE-2010 microscope operated at 200 kV.

The particle size of Pt NPs in the Pt (60 wt%)/SDS–MWCNTs was determined by a X-ray diffraction (XRD) pattern, which was obtained on a Rigaku 1200 by using Cu-Kα radiation, a Ni β-filter and operating at 40 kV and 20 mA.

X-ray photoelectron spectroscopy (XPS) analysis was carried out with an AXIS-NOVA (Kratos) X-ray photoelectron spectrometer using monochromated Al Kα (150 W) source under base pressure of 2.6×10^{-9} Torr.

2.3. Catalyst electrode preparation, characterization and fuel cell performance

Prior to the preparation of catalyst ink for the fabrication of catalyst electrodes and for the electrochemical measurements, the SDS–MWCNT-supported Pt catalyst was heated at 450 °C for 3 h under N_2 flow to remove the residual SDS.

A three-electrode electrochemical cell was constructed for cyclic voltammetric (CV) measurements, through which the electrochemical surface areas (ECSAs) of the Pt in Pt (60 wt%)/SDS–MWCNTs (HD-EG) and in Pt (60 wt%)/VC (J. M.) were determined. CV measurements were conducted at room temperature in 0.5 M H_2SO_4 with a scan rate of 25 mV s^{-1}. For the electrochemical measurements, a Pt gauze was used as a counter electrode and Ag/AgCl as the reference electrode. The electrolyte solution was deaerated with high-purity nitrogen for 1 h prior to any cyclic voltammetric measurement and stable voltammograms were recorded after 10 cycles. The working electrode was a thin layer of Nafion-impregnated catalyst, cast on a glassy carbon disk of 3 mm in diameter embedded in a Teflon cylinder. The details for the fabrication of the catalyst layer can be seen elsewhere.[29] Single cells were constructed for the evaluation of the polarization performance of the fuel cells based on various Pt (60 wt%)/C cathode catalysts, *i.e.* Pt (60 wt%)/SDS–MWCNT (HD-EG) and Pt (60 wt%)/VC (J. M.). A membrane electrode assembly (MEA) with an area of 6.25 cm^2 was used to construct a single cell, which had been fabricated by hot-pressing a pre-treated Nafion 112 (Du-Pont) sandwiched between the anode and cathode. The catalyst loadings were 0.4 and 0.2 mg cm^{-2} of Pt at the anode and cathode, respectively. Pt (20 wt%)/VC (E-TEK) was used as the anode catalyst. The catalyst electrodes for the single cell tests were prepared by painting an appropriate amount of the catalyst inks uniformly on Teflonized carbon paper (TGPH-090) and dried at 80 °C overnight. The catalyst inks were prepared by dispersing various Pt/C catalysts into a solution composed of an appropriate amount of DI water and the required amount of 5 wt% Nafion ionomer solution (Aldrich). The Nafion ionomer contents were 20 and 25 wt% in the anode and cathode catalyst layer, respectively. The polarization performance of the fuel cells were examined at 60 °C under constant current or constant voltage with a WFCTS fuel cell test station, after they were humidified at 75 °C. H_2 and O_2 were supplied to the anode and cathode at a flow rate of 200 and 500 mL min^{-1}, respectively.

3. Results and discussion

3.1. Pt loading on MWCNTs by various synthetic strategies

The loading of Pt NPs onto the MWCNT was realized through various synthetic strategies including: 1) a urea-assisted HD-EG strategy for the as-received MWCNTs, 2) the strategy using SDS as both the protective and the reducing agent, 3) the impregnation strategy using $NaBH_4$ as the reducing agent (pH = 8), 4) the microwave-assisted polyol process using EG as the reducing agent (*i.e.*, EG-MW) (pH = 8) and 5) a urea-assisted HD-EG strategy for the SDS–MWCNT. The HD-EG strategy has been proven to be very effective in preparing VC-supported Pt-based catalysts with high metal loading.[29] However, as is evident from Fig. 1a, the HD-EG strategy does not demonstrate a uniform Pt NPs dispersion on the as-received MWCNTs (*i.e.*, without any post-treatment). In addition, TGA, shown in Fig. S1 in the electronic supplementary information (ESI),† reveals a Pt loading of *ca.* 27 wt% for this catalyst, which is much less than the set value (*i.e.* 40 wt%). The poor Pt loading is mainly attributable to the high chemical inertness of pristine MWCNTs, making it difficult to anchor and deposit the Pt NPs. The result also implies that a surface modification is necessary for the MWCNTs to support high loading of Pt.

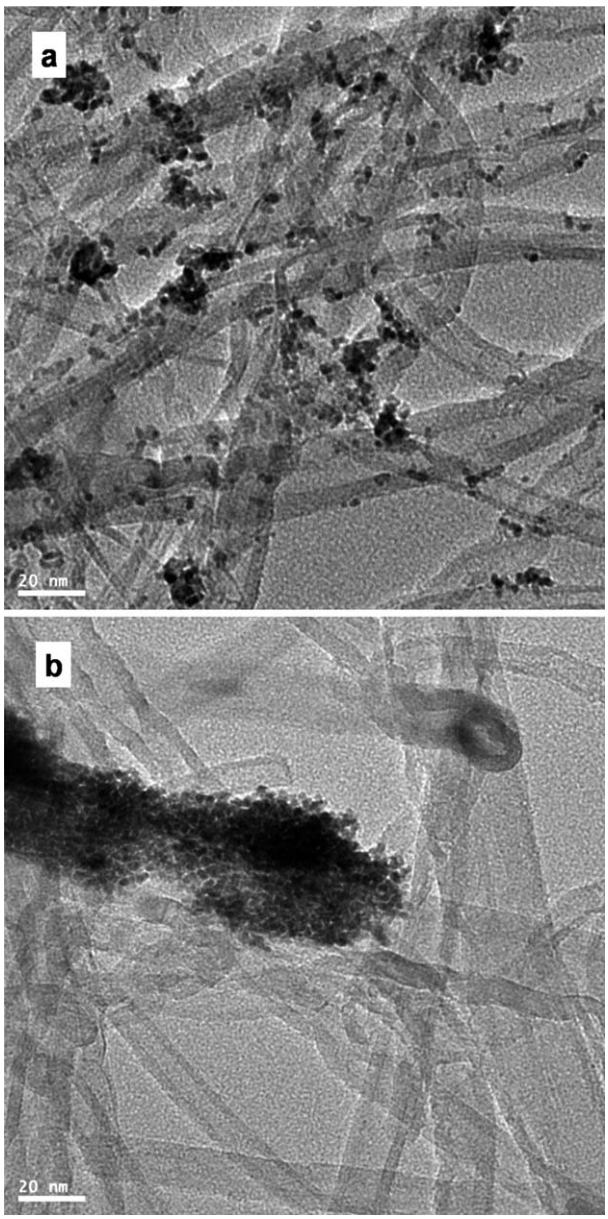

Fig. 1 Representative TEM images for the MWCNT-supported Pt catalysts with a nominal metal loading of 40 wt%: (a) synthesized by the urea-assisted HD-EG strategy and (b) synthesized by using SDS as the reducing agent.

SDS has been reported to be very efficient as a non-covalent stabilizer to improve the adsorption of Pt(IV) species on MWCNT supports. Lee *et al.*[39] claimed that SDS could not only serve as a stabilizer to modify the surface structure of MWCNTs, but also as a reducing agent (the precursor/resource of a reducing agent) for the deposition of Pt metal, so there was no need for the introduction of an external reducing agent. Unfortunately, SDS does not work as well as expected. Evidently from Fig. 1b, Pt NPs do not disperse homogenously on the MWCNT support. Also, the TGA, shown in Fig. S1 in the ESI†, reveals a very low Pt loading (*ca.* 31 wt%) for this catalyst. The poor dispersion of the Pt NPs on the support observed for this strategy is probably attributable to the existence of excess SDS in the bulk solution containing the Pt(IV) species, making the reduction of the Pt(IV) species take place everywhere (*i.e.* not only on the SDS-coated MWCNTs, but also in the bulk solution). Thus, it seems unsuitable for SDS to play the two roles, as a stabilizer and a reducing agent at the same time. As a surfactant, it is effective as a stabilizer. For this reason, in our study and from then on, SDS only served as a stabilizer to functionalize the MWCNTs. SDS-modified MWCNTs (*i.e.*, SDS–MWCNTs) were used as a support for moderate/high Pt loading (*i.e.* 40 or 60 wt%) and, to achieve the goal of homogeneous dispersion of the Pt NPs, different reducing agents and catalyst synthetic strategies were explored. The SDS content in the SDS–MWCNTs is *ca.* 5 wt%, as revealed by the TGA profiles shown in Fig. S2 in the ESI.†

Fig. 2 presents the typical TEM images for the SDS–MWCNT-supported Pt catalysts prepared using different reducing agents and catalyst synthetic strategies. Although the TGA profiles (Fig. S1 in the ESI†) do not reveal much difference in the Pt loadings between these catalysts (*i.e.* 35 wt%, 37 wt% and 39 wt% for $NaBH_4$, EG-MW and HD-EG catalysts, respectively), differences can be clearly seen in their TEM images, shown in Fig. 2. The catalyst synthesized using $NaBH_4$ as the reducing agent under pH = 8 reveals the worst Pt NP dispersion on the SDS–MWCNT support, as shown in Fig. 2a. This may suggest that *ex situ* addition of the reducing agent $NaBH_4$ cannot guarantee the homogeneous reduction of the Pt(IV) complex species anchored on the SDS–MWCNTs, and some of Pt NPs produced with a small size may agglomerate into larger sized NPs during the reduction process, which is probably attributable to the strong reducing ability of $NaBH_4$ at room temperature. In addition, a local pH increase in the solution may be involved in the step of pH adjustment realized through *ex situ* dropwise addition of 0.4 M KOH, resulting in uneven dispersion of the Pt NPs. In contrast, a more homogeneous reduction of the Pt(IV) complex species on the SDS–MWCNTs took place through the *in situ* generation of the reducing agent from the microwave-assisted EG process, as evident from Fig. 2b, which reveals

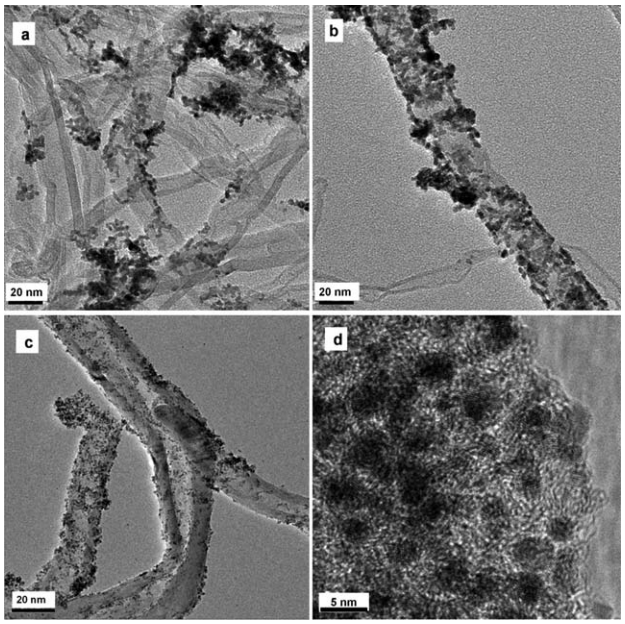

Fig. 2 Representative TEM images of SDS–MWCNT supported Pt catalysts with a nominal metal loading of 40 wt%: synthesized (a) using $NaBH_4$ as the reducing agent at pH = 8, (b) by EG-MW at pH = 8, (c) by urea-assisted HD-EG and (d) a higher magnification image of the catalyst shown in (c).

a more uniform dispersion of Pt NPs on the support. Interestingly, compared with the two catalysts prepared at pH = 8 (in both cases they were realized through *ex situ* dropwise addition of 0.4 M KOH), the SDS–MWCNT-supported Pt (40 wt%) catalyst prepared by the urea-assisted HD-EG approach demonstrates a much more uniform dispersion of Pt NPs on the support with smaller particle size, and there is no obvious agglomeration observed for this catalyst, as is made clear from their TEM images, shown in Figs 2c and d. Evidently, the difference between the catalyst prepared by EG-MW under pH = 8 and that by urea-assisted HD-EG should be mainly attributable to the difference in the techniques used to control the pH. As reported by Fang *et al.*,[29] pH has very important impact on the particle size and distribution of the supported Pt NPs. An external addition of KOH (*i.e.* OH^-) into the solution cannot guarantee a gradual and even increase in the pH value, and local pH increases in the solution may occur, which may result in a variation in Pt(IV) complex species and thus in the size and distribution of the Pt NPs on the support during the reduction step. As for the SDS–MWCNT-supported Pt catalyst prepared by the urea-assisted HD-EG approach, the urea-assisted HD step allows *in situ* generation of OH^- through the hydrolysis of urea at an elevated temperature and a gradual increase in the pH value, while the EG reduction step allows *in situ* generation of a reducing agent through the decomposition of EG at an elevated temperature. In the urea-assisted HD process, the urea in the acidic Pt salt solution hydrolyzes as follows to gradually generate OH^- homogeneously throughout the solution: $CO(NH_2)_2 + 3H_2O \rightarrow 2NH_4^+ + CO_2 + 2OH^-$. *In situ* generation of OH^- guarantees homogenous deposition of the Pt(IV) complex species with a uniform and small size on the SDS–MWCNT support, while *in situ* generation of the reducing agent ensures the simultaneous reduction of the deposited Pt(IV) complex species, further guaranteeing the uniform distribution of Pt NPs on the catalyst support. In addition, because urea contains amine groups, which have a good binding ability to Pt, urea might also interact with Pt salt to form Pt(IV) complex species, improving the level of Pt loading on the MWCNTs. Further work is needed to confirm the effects of urea.

3.2. High Pt loading on SDS–MWCNTs by HD-EG strategy

Supported high Pt loading catalyst with uniform Pt NP dispersion and small particle size is highly desired in PEMFCs due to the expected fast mass transport through the thin catalyst layer and reduced cost in the catalyst support (a lower amount of the catalyst support is required compared with a low Pt loading catalyst). However, it still remains a major challenge in synthesizing high Pt loading catalysts, particularly on CNT supports, which are chemically inert if there is no activation for their graphitic surface. In most publications, Pt loadings on CNT supports were rather low, usually less than 20 wt%. Inspired by the successful preparation of SDS–MWCNT-supported Pt (40 wt%) catalysts through the urea-assisted HD-EG approach, in this study, a synthesis of a SDS–MWCNT-supported Pt catalyst with higher metal loading, namely, 60 wt%, was attempted.

Fig. 3a and b show representative HRTEM images for the SDS–MWCNT-supported Pt (60 wt%) catalyst prepared by the urea-assisted HD-EG strategy. The TGA shown in Fig. S1 in the ESI† reveals a metal loading of *ca.* 57 wt% for this catalyst, which is very close to the nominal value, implying complete adsorption of Pt(IV) species on the SDS–MWCNT surface. Compared with the SDS–MWCNT-supported Pt (40 wt%) catalyst prepared using the same strategy, the dispersion of Pt NPs on the support still remains very uniform, while the particle size for the former catalyst is slightly larger. Evidently, the effect from the surface functionalization by SDS is significant. When MWCNTs are functionalized by anionic SDS surfactant, the hydrophobic ends of the SDS molecules face toward and attach to the surface of the MWCNTs, while the hydrophilic groups (*i.e.* SO_4^-) are usually in contact with the polar surroundings (*i.e.* water), giving good dispersion of MWCNTs in an aqueous medium,[42] which favours high Pt loading on the MWCNT support with a uniform dispersion of Pt NPs.

From Fig. 3a and Fig. S3a (ESI†), it was found that some MWCNTs are not well coated with Pt NPs, particularly MWCNTs with smaller diameters, usually those that are less than 10 nm. This phenomenon was also observed for MWCNTs with small diameters in another publication.[44] While on MWCNTs with larger diameters, Pt NPs distribute uniformly on the whole outer surface, as is evident in Fig. 3a and Fig. S3b (ESI†). In the case of MWCNTs with smaller diameters, the poor Pt loading may be mainly attributable to insufficient surface area for the homogeneous deposition of high loading of Pt NPs. As we know, a large surface area is a basic requirement for a catalyst support to have a uniform distribution of metal NPs. In addition, other factors, such as heating time and temperature, may have an important influence on the Pt loading on the support. Sakthivel *et al.* reported that when EG was used as a reducing agent, the Pt catalyst obtained at a higher heating temperature (*i.e.* 140 °C)

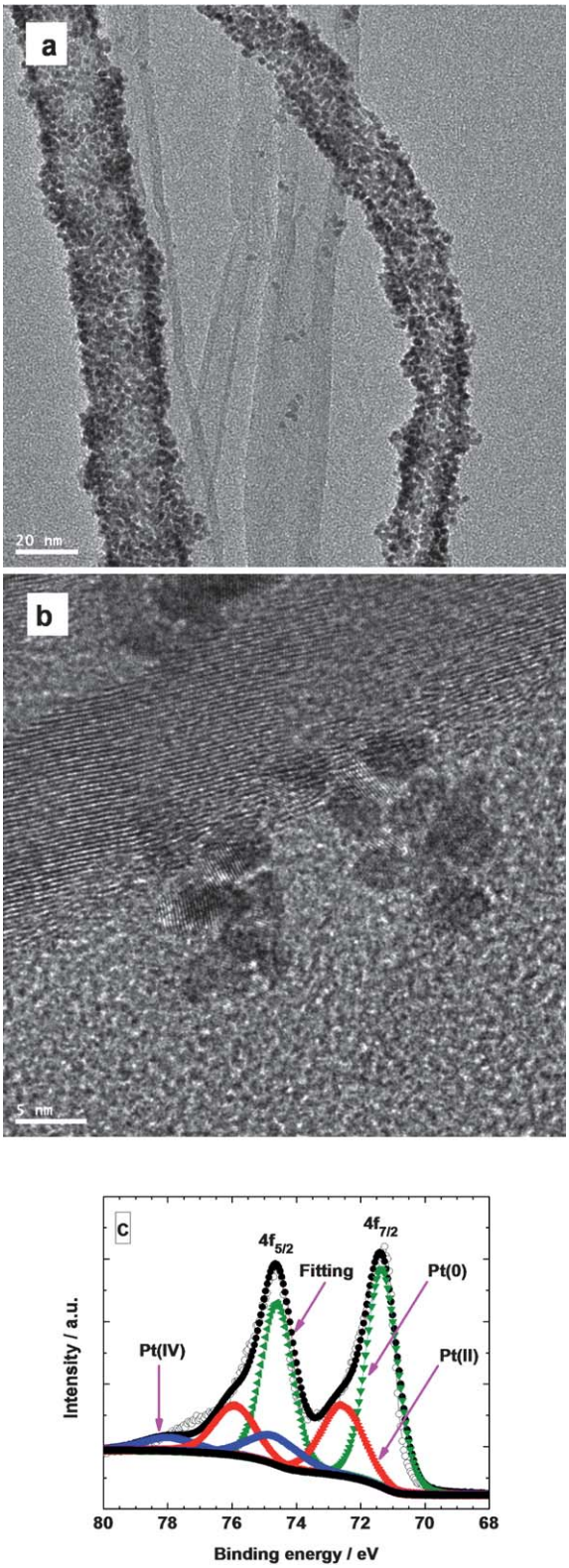

Fig. 3 Representative HRTEM images (a and b) and XPS (c) for the SDS–MWCNT supported Pt (60 wt%) catalyst synthesized by the urea-assisted HD-EG strategy.

had a better distribution of Pt NPs than that at 120 °C.[45] At present, the mechanism of the poor Pt loading on some SDS–MWCNTs is not very clear about, and future works, such as investigation into the effect of the heating temperature, heating time and the SDS loading on MWCNTs, are planned to perfect the synthesis strategy developed in this study. Fig. 3b reveals that the Pt NPs have particle sizes of *ca.* 2.5–4.1 nm. The XRD pattern shown in Fig. S4 (ESI†) exhibits characteristics of a Pt face-centered cubic structure and reveals an average particle size of *ca.* 3.0 nm for the SDS–MWCNT-supported Pt (60 wt%) catalyst, which was calculated using a Debye–Scherrer equation from the broadening of the Pt (220) reflection.[46] The calculated size of the Pt NPs from XRD is basically in agreement with the direct measurements from the HRTEM image shown in Fig. 3b. From the XPS spectra in the Pt 4f region, shown in Fig. 3c, doublet peaks were observed at 71.4 and 74.7 eV, which are attributable to $4f_{7/2}$ and $4f_{5/2}$ of metallic Pt, respectively, indicating that the dominant valence of the Pt species in the SDS–MWCNT-supported Pt (60 wt%) catalyst is zero. From the deconvoluted curves, the composition of Pt in the catalyst is calculated to be 76% of Pt(0), 16% of Pt(II) and 8% of Pt(IV). This composition suggests a basically complete reduction of the adsorbed Pt(IV) complex species by the EG, implying that the urea-assisted HD-EG strategy is highly efficient for the preparation of high Pt loading catalyst with an SDS–MWCNT support.

3.3. ECSA and fuel cell polarization performance for SDS–MWCNT- or VC-supported Pt (60 wt%) catalysts

ECSA is a very significant parameter reflecting the intrinsic electrocatalytic activity of a Pt catalyst, which is usually determined by the integrated charge (after subtraction of the capacitance contribution) in the hydrogen absorption region of the steady-state cyclic voltammogram in a supporting electrolyte (*i.e.* 0.5 M H_2SO_4), based on a monolayer hydrogen adsorption charge of 0.21 mC cm^{-2} on polycrystalline Pt. Fig. 4a presents H-electrosorption profiles in 0. 5 M H_2SO_4 at 25 mV s^{-1} for various carbon-supported Pt (60 wt%) catalysts, *i.e.* SDS–MWCNT-supported Pt (60 wt%) catalysts prepared by the HD-EG approach and commerical Pt (60 wt%)/VC (J. M.). ECSAs are calculated to be 83 and 56 m^2 g^{-1} for the SDS–MWCNT-supported Pt (60 wt%) catalyst (HD-EG) and Pt (60 wt%)/VC (J. M.), respectively. The much higher ECSA of the SDS–MWCNT-supported catalyst is attributable to a more uniform dispersion of the Pt NPs on the support with a smaller particle size (particle size of Pt (60 wt%)/VC (J. M.) is *ca.* 3.2 nm[29]). In addition, the high conductivity of MWCNTs and the one dimensional nanostructure of CNTs favoring fast electron transfer also contribute much to the considerably enhanced ECSA.

Fuel cell polarization plots for various Pt (60 wt%) cathode catalysts are shown in Fig. 4b. For H_2-fueled PEMFC, the polarization in the low current density region is electrochemical-activation controlled and caused primarily by the sluggish ORR at the cathode. In the low current density region, the intrinsic electrocatalytic property of the electrode can be clearly observed without the interruption of ohmic loss and the mass transfer phenomenon. Compared with Pt (60 wt%)/VC (J. M.), a smaller loss in the polarization voltage was observed for the SDS–MWCNT-supported Pt (60 wt%) (HD-EG) catalyst, implying a higher electrocatalytic activity toward ORR for the latter.

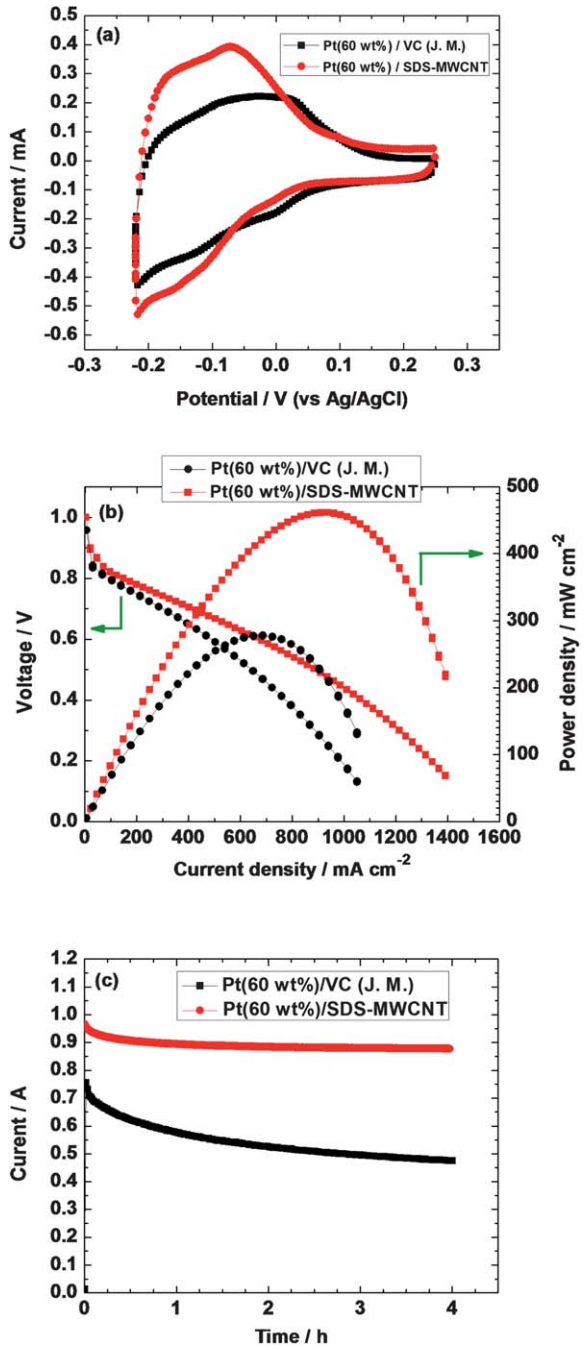

Fig. 4 H-electrosorption profiles in 0.5 M H_2SO_4 (a), fuel cell polarization plots at 60 °C (b) and chronoamperograms obtained at 0.75 V (c) for the SDS–MWCNT-supported Pt (60 wt%) catalyst prepared by the HD-EG strategy and VC-supported Pt (60 wt%) (J. M.).

Furthermore, the SDS–MWCNT-supported Pt (60 wt%) (HD-EG) catalyst demonstrates a maximum power density of 451 mW cm^{-2}, which is much higher than that for the Pt (60 wt%)/VC (J. M.) (*i.e.* 276 mW cm^{-2}). From the chronoamperograms obtained at 0.75 V shown in Fig. 4c, it can be clearly observed that the SDS–MWCNT-supported Pt (60 wt%) (HD-EG) catalyst reveals a much higher current response and higher electrochemical stability than the Pt (60 wt%)/VC (J. M.). The superior catalytic activity and fuel cell polarization performance for the SDS–MWCNT-supported Pt catalyst is attributable to its larger ECSA, the high electronic conductivity of MWCNTs and the one dimensional nanostructure of CNTs facilitating rapid electron transfer. The higher catalytic activity and much better fuel cell performance demonstrated by the SDS–MWCNT catalyst prepared by the urea-assisted HD-EG strategy suggest that the synthetic strategy developed in this study is highly efficient.

4. Conclusions

In this study, a simple but very efficient synthesis strategy has been developed for high loading of Pt on MWCNTs. Through the non-covalent surface functionalization by SDS, large quantities of homogeneously distributed active sites can be generated for anchoring Pt(IV) species. Furthermore, this mild surface modification preserves the intrinsic properties of the MWCNTs. The HD-EG strategy provides a gradual and homogeneous increase in pH through the *in situ* hydrolysis of urea at an elevated temperature, resulting in homogeneous deposition of Pt (IV) complex species on the MWCNT support, while the *in situ* generation of reducing agent from the decomposition of EG further guarantees homogenous reduction of the adsorbed Pt(IV) complex species on the MWCNT support. The observed remarkable enhancement in the Pt deposition efficiency, together with the homogeneity, are attributable to the synergy of SDS, the homogeneous deposition of Pt(IV) complex species through the *in situ* hydrolysis of urea, and the homogeneous reduction of Pt(IV) complex species by the reducing agent generated *in situ* from EG.

Compared with a commerical Pt (60 wt%)/VC (J. M.) catalyst, a higher catalytic activity toward ORR and a much better fuel cell performance have been demonstrated by the SDS–MWCNT-supported Pt (60 wt%) catalyst prepared by the urea-assisted HD-EG strategy, which is mainly attributable to a more uniform dispersion of Pt NPs on the support, along with a smaller particle size. In addition, high conductivity and the one-dimensional nature of the MWCNTs also contribute something to the enhanced fuel cell performance due to faster electron transfer.

The results presented in this study highlight the following findings: an ability to achieve high Pt loading on MWCNTs with a uniform dispersion of Pt NPs and a small particle size through the non-covalent surface functionalization of MWCNTs, *in situ* adjustment of pH and *in situ* generation of reducing agent. The strategy developed in this study is relatively simple (*i.e.* not many steps are involved and little time is consumed), cost effective (*i.e.* the usage of Pt catalysts can be reduced considerably due to the remarkable enhancement of the utilization of Pt in the catalyst compared to commercial Pt (60 wt%)/VC (J. M.) catalyst) and reproducible, implying that the synthetic strategy is promising for commercialization after the optimization of the synthesis conditions. In addition, this strategy is expected to extend its application to the preparation of other high loading Pt-based alloy catalysts, non-noble metal catalysts, and catalysts of metal NPs deposited on other support materials, such as CNF. This study is in progress.

Acknowledgements

This work was supported by the KRF grant funded by the Korean government (KRF 2010-0029245) and Human

Resources Development Program (2009) of KETEP. The authors would also like to thank the Korean Basic Science Institute at Jeonju and Chuncheon for SEM and TEM analyses.

References

1 N. Tian, Z.-Y. Zhou, S.-G. Sun, Y. Ding and Z.-L. Wang, *Science*, 2007, **316**, 732.
2 R. Borup, J. Meyers, B. Pivovar, Y.-S. Kim, R. Mukundan, N. Garland, D. Myers, M. Wilson, F. Garzon and D. Wood, *Chem. Rev.*, 2007, **107**, 3904.
3 B.-Z. Fang, J.-H. Kim, C.-G. Lee and J.-S. Yu, *J. Phys. Chem. C*, 2008, **112**, 639.
4 B.-Z. Fang, J.-H. Kim and J.-S. Yu, *Electrochem. Commun.*, 2008, **10**, 659.
5 J.-H. Kim, B.-Z. Fang, M.-S. Kim, S.-B. Yoon, T.-S. Bae, D. R. Ranade and J.-S. Yu, *Electrochim. Acta*, 2010, **55**, 7628.
6 M.-S. Kim, S.-H. Hwang and J.-S. Yu, *J. Mater. Chem.*, 2007, **17**, 1656.
7 B.-Z. Fang, M.-S. Kim, S.-H. Hwang and J.-S. Yu, *Carbon*, 2008, **46**, 876.
8 G. Wu, C.-S. Dai, D.-L. Wang, D.-Y. Li and N. Li, *J. Mater. Chem.*, 2010, **20**, 3059.
9 B.-Z. Fang, M.-S. Kim and J.-S. Yu, *Appl. Catal., B*, 2008, **84**, 100.
10 J.-H. Kim, B.-Z. Fang, S.-B. Yoon and J.-S. Yu, *Appl. Catal., B*, 2009, **88**, 368.
11 J.-H. Kim, B.-Z. Fang, M.-W. Kim and J.-S. Yu, *Catal. Today*, 2009, **146**, 25.
12 P. W. Park, B. K. Kwon, J. H. Choi, I. S. Park, Y. M. Kim and Y. E. Sung, *J. Power Sources*, 2002, **109**, 439.
13 G. Girishkumar, M. Retter, R. Underhile, D. Binz, K. Vinodgopal, P. McGinn and P. Kamat, *Langmuir*, 2005, **21**, 8487.
14 K.-C. Lee, J.-J. Zhang, H.-J. Wang and D. P. Wilkinson, *J. Appl. Electrochem.*, 2006, **36**, 507.
15 D.-J. Guo and H.-L. Li, *J. Electroanal. Chem.*, 2004, **573**, 197.
16 M. Zhang, Y. Yan, K. Gong, L. Mao, Z. Guo and Y. Chen, *Langmuir*, 2003, **20**, 8781.
17 F.-L. Yuan and H. Ryu, *Nanotechnology*, 2004, **15**, S596.
18 L. Zhang, B. Cheng and E. T. Samulski, *Chem. Phys. Lett.*, 2004, **398**, 505.
19 M. Gangeri, G. Centi, A. La Malfa, S. Perathoner, R. Vieira, C. Pham-Huu and M. J. Ledoux, *Catal. Today*, 2005, **102–103**, 50.
20 B.-Z. Fang, J.-H. Kim, M.-S. Kim, M.-W. Kim and J.-S. Yu, *Phys. Chem. Chem. Phys.*, 2009, **11**, 1380.
21 B.-Z. Fang, J.-H. Kim, M.-S. Kim and J.-S. Yu, *Chem. Mater.*, 2009, **21**, 789.
22 E. S. Steigerwalt, G. A. Deluga and C. M. Lukehart, *J. Phys. Chem. B*, 2002, **106**, 760.
23 K.-Y. Chan, J. Ding, J. Ren, S. Cheng and K. Y. Tsang, *J. Mater. Chem.*, 2004, **14**, 505.
24 C. Bock, C. Paquet, M. Couillard, G. A. Botton and B. R. MacDougall, *J. Am. Chem. Soc.*, 2004, **126**, 8028.
25 C. M. Y. Yeung, K. M. K. Yu, Q.-J. Fu, D. Thompsett, M. I. Petch and S. C. Tsang, *J. Am. Chem. Soc.*, 2005, **127**, 18010.
26 W.-Y. Yu, W.-X. Tu and H.-F. Liu, *Langmuir*, 1999, **15**, 6.
27 Z.-L. Liu, J.-Y. Lee, W.-X. Chen, M. Han and L.-M. Gan, *Langmuir*, 2004, **20**, 181.
28 G.-S. Chai, B.-Z. Fang and J.-S. Yu, *Electrochem. Commun.*, 2008, **10**, 1801.
29 B.-Z. Fang, N.-K. Chaudhari, M.-S. Kim, J.-H. Kim and J.-S. Yu, *J. Am. Chem. Soc.*, 2009, **131**, 15330.
30 M.-S. Kim, B.-Z. Fang, N. K. Chaudhari, M.-Y. Song, T.-S. Bae and J.-S. Yu, *Electrochim. Acta*, 2010, **55**, 4543.
31 J. Chen, M. A. Hamon, H. Hu, Y. Chen, A. M. Rao, P. C. Eklund and R. C. Haddon, *Science*, 1998, **282**, 95.
32 Y.-C. Xing, *J. Phys. Chem. B*, 2004, **108**, 19255.
33 Y.-C. Xing, L. Li, C. C. Chusuei and R. V. Hull, *Langmuir*, 2005, **21**, 4185.
34 X. Wang, W.-Z. Li, Z.-W. Chen, M. Waje and Y.-S. Yan, *J. Power Sources*, 2006, **158**, 154.
35 S.-Y. Wang, X. Wang and S.-P. Jiang, *Langmuir*, 2008, **24**, 10505.
36 P. Santhosh, A. Gopalan and Kwang-Pill Lee, *J. Catal.*, 2006, **238**, 177.
37 J.-H. Zhou, J.-P. He, Y.-J. Ji, W.-J. Dang, X.-L. Liu, G.-W. Zhao, C.-X. Zhang, J.-S. Zhao, Q.-B. Fu and H.-P. Hu, *Electrochim. Acta*, 2007, **52**, 4691.
38 S.-Y. Wang, S.-P. Jiang, T. J. White, J. Guo and X. Wang, *J. Phys. Chem. C*, 2009, **113**, 18935.
39 C.-L. Lee, Y.-C. Ju, P.-T. Chou, Y.-C. Huang, L.-C. Kuo and J.-C. Oung, *Electrochem. Commun.*, 2005, **7**, 453.
40 B.-H. Wu, D. Hu, Y.-J. Kuang, B. Liu, X.-H. Zhang and J.-H. Chen, *Angew. Chem., Int. Ed.*, 2009, **48**, 4751.
41 R. Menzel, M. Q. Tran, A. Menner, C. W. M. Kay, A. Bismarck and M. S. P. Shaffer, *Chem. Sci.*, 2010, **1**, 603.
42 C.-L. Lee, C.-C. Wan and Y.-Y. Wang, *Adv. Funct. Mater.*, 2001, **11**, 344.
43 X.-G. Li and I.-M. Hsing, *Electrochim. Acta*, 2006, **51**, 5250.
44 L. Cao, F. Scheiba, C. Roth, F. Schweiger, C. Cremers, U. Stimming, H. Fuess, L.-Q. Chen, W.-T. Zhu and X.-P. Qiu, *Angew. Chem., Int. Ed.*, 2006, **45**, 5315.
45 M. Sakthivel, A. Schlange, U. Kunz and T. Turek, *J. Power Sources*, 2010, **195**, 7083.
46 J. L. Fernandez, D. A. Walsh and A. J. Bard, *J. Am. Chem. Soc.*, 2005, **127**, 357.